Volume 15, Number 1, 2022. pp. 49-56

Jordan Journal of Physics

ARTICLE

Optical, Structural and Electrical Properties of CuS Thin Film on Dielectric Substrate by Spray Pyrolysis Technique

Avish K. Patil[a], Sachin H. Dhawankar[b], Nishant T. Tayade[c]

[a] *Department of Physics, DRB Sindhu Mahavidyalaya, Panchpaoli, Nagpur, Maharastra, India.*

[b] *Department of Physics, Shri JSPM Arts, Commerce and Science College, Dhanora - 442606, Gadchiroli, Maharashtra, India.*

[c] *Department of Physics, Institute of Science, (Formerly) Nagpur, Maharastra, India.*

Doi: **https://doi.org/10.47011/15.1.7**

Received on: 01/08/2020 *Accepted on: 17/01/2021*

Abstract: This paper deals with depositing a CuS thin film on a glass substrate at 380^{0}C by using spray pyrolysis method. Its optical properties and electric properties are characterized after cooling the sample. Formation for compound, structure and morphology were studied using x-ray diffraction. The optical study comprised the extraction and analysis of calculated optical constants, such as absorption coefficient (α), transmittance, extinction coefficient (k), which revealed the presence of a direct optical energy band gap of 2.0 eV. The temperature-dependent electrical resistivity with other necessary parameters was systematically studied for CuS film in the present work. Overall study confirmed the semiconducting behavior of the film which is useful for many applications, even when the film is touching the substrate at a micrometer scale with spray pyrolysis. This paper also explores the optical conductivity, dielectric constant, Urbach energy, morphology and thermal activation energy of the CuS film with explaining methodological details.

Keywords: Thin film, Spray pyrolysis technique, Electrical and optical properties, XRD.

Introduction

The CuS metal thin film belongs to I – VI compound semiconductor materials. It is used in several applications, such as microwave shielding, photo thermal, photo detector, photovoltaic and solar control coating applicationsas well as its uses as a wide-energy gap semiconductor and as an electro conductive electrode … etc [1-5]. Such metal thin films also have applications in diamond d films, magnetic films, superconducting films, microelectronic devices, surface modification, hard coating, photoconductors, IR detectors, optical imaging, optical mass memories and sensors [3-6]. Different types of methods are used for thin-film deposition, such as chemical bath deposition [4-6], spray pyrolysis [7], successive ionic layer absorption and reaction [1], electrode position [8], atomic layer deposition [9-10], sol gel [11-13] and solution growth [14-15].

The optical band gap energy (Eg) of Cu_XS thin films for 3D solar cell applications has been reported to be 2.41 to 3.1 eV with crystalline phase and found to be temperature-dependent [2]. The thin film exhibited polycrystalline structure when substrate temperature reached 320°C. Direct energy band gap has been reported to be 2.07 to 2.50eV in another work. Cu_xS thin films possess p-type semiconducting behavior [3]. Nascu studied at 150 to 220°C deposited, 0.01 to 0.05μm thickness films and found a 2.2 eV bandgap [16].Adelifard *et al*. reported 2.4 to 2.6eV for substrate temperatures 250, 285 and

Corresponding Authors: S. H. Dhawankar **Emails**: sachindhawankar@gmail.com
N. T Tayade nishanttayade@rediffmail.com

310°C [17]. Firat *et al.* also reported Eg of 2.07 eV for 320°C [18]. For the 380°C substrate temperature-deposited CuS thin film, it is expected to show some changes in structure and optical properties as evident from an overview of previous reports [2, 3, 19]. We observed in literature that the CuS film has not been optically characterized immediately after its synthesis and cooling to room temperature.

Therefore, we proposed to conduct this work to test the optical and electrical properties immediately after the cooling down (to room temperature) of CuS thin film deposited on a glass slide at 380°C substrate temperature. For that, the simple, fast growing, low-cost and convenient deposition spray pyrolysis technique was used.

Experimental Details

Synthesis of CuS Thin Film

The substrate of glass plate was cleaned before depositing the CuS thin film on it. A glass slide was taken as a substrate and it was cleaned with nitrate acid (conc.) for 3 hours, then rinsed with double distilled water and kept in ultrasonicator for several times to remove the impurities on the surface. The cleaned glass slide was weighed before and after deposition using an electron unipan microbalance. For accuracy concerns, four batches of 10 readings were taken and the average was obtained by statistical methods.

The film had been prepared by the following chronological order. The aqueous solution for deposition of CuS thin film consisted of copper chloride (1N) and thiourea (1N) dissolved in double distilled water separately and stirred for 10-12 hours to form a clear solution. Equal amounts of both solutions were mixed and kept stirring for 3 hours. The cleaned glass slide was arranged to use spray pyrolysis for deposition of CuS thin film at 380^0C. After the finish of deposition part, the glass slide was allowed to cool at room temperature. The thickness of CuS thin film is calculated by using the weight difference density method (discussed in a previous paragraph) which is the most convenient method to calculate the thickness of thin film.

Spray pyrolysis deposition was done by using a laboratory-designed glass atomizer, which has an output nozzle of <1 mm. The period between spraying processes was about 2 to 3 min. This period is enough to avoid excessive cooling of the glass substrate. The carrier gas (compressed air) was maintained at a pressure of 100 Nm^2. Distance between nozzle and substrate was about 30 cm and solution flow rate was 5 ml/min. The five sample slides were prepared this way and immediately characterized for optical study using manual microscopic observation to select good films by surface uniformity and the best CuS thin film was selected for the full study first using electrical characterization and then XRD characterization.

Characterization Methods

Thin film was characterized by XRD preferentially to check whether the CuS phase was successfully formed or not formed. XRD data was recorded from 20 to 60 degrees for the Cu Kα radiation of 1.54060 Å. The indexing information (and plot provided by technician along with background subtraction) was post-processed manually for the unit cell refinement using the CELREF software, rendering the calculation for microstructure.

Optical characterization was conducted immediately after the cooling of the prepared thin film to room temperature. Optical properties of the deposited CuS thin film were studied by using UV – VIS Spectrophotometer (ELCO SL-159) at wavelengths ranging from 380 – 1000 nm, using four-probe technique. Optical absorption spectra of CuS thin film are studied on ELCO – SL 159 UV – VIS Spectrophotometer in the optical range from 380to1000 nm.

A high-impedance digital electrometer KEITHLEY 6514 system was used to measure the floating potential between second and fourth probes of the four-probe apparatus. 'DFP 03' oven was used to adjust the temperature for the range from 300K to 380K. K-type thermocouple with accuracy of 0.75% above 400K was used to measure temperature. The AGRONIC-92D was used as a constant-current source for this system.

Results and Discussion

Thickness of Thin Film

The thickness of CuS thin film was estimated at 1.0973 μm. The thickness (d) is calculated from Eq. (1) using the mass of the film (M) deposited on the substrate, where $\rho$is the density of the deposited substance and A is the area of the deposited film.

$$d = \frac{M}{\rho A} \quad (1)$$

Structure by XRD

X-ray diffraction pattern is shown in Fig. 1. The prominent and good peaks were indexed to (102), (103), (006), (110) and (116), which confirms the formation of hexagonal phase. The symmetry has been found present for the 194 space group, which is also indicated by H-M standard symbol P63/mmc (Hall symbol –P 6C 2C). These patterns seem to be likely in agreement with JCPDS Card Number 06 – 0464.Broadening of peak and very large background noise proposes the nano-dimension case and confirms the crystallites or grains having nano size at microstructure. It is well known that the thin film is confined into one direction in nm size. Thus, characterization confirms the formation of polycrystalline CuS compound deposited on the substrate as a thin film. The unit cell refinement reveals its lattice parameters, volume and density as presented in Table 1 and details of analysis are given in a supplement as Table S1. All values are comparatively slightly lower values than in the work done for 320°C [18]. Our results are found slightly shifting to lower 'a' and 'c' constants of the TF1 sample in the paper. This confirms that close packing is tight. The zero error correction has been also done in refinement and was found to be -0.520 further reduction in the volume of unit cell.

TABLE S1. XRD outcomes of refinement at final cycle of iteration.

(a): Refined Parameters

Parameters	Zero	a	b	c	alpha	beta	gamma	volume
Value	-0.520	3.7738	3.7738	16.3431	90.00	90.00	120.00	201.57
Std. Error	0.0393	0.0084	0.0000	0.1104	0.000	0.000	0.000	1.434

(b): Corrected 2Th corresponding to hkl planes

h	k	l	2Th(obs)	2Th_obs-shift	2Th(Calc)	diff.
0	1	2	28.8900	29.3936	29.3939	-0.0003
0	1	3	31.3560	31.8567	31.8874	-0.0307
0	0	6	32.3730	32.8724	32.8339	0.0385
1	1	0	47.7100	48.1856	48.1433	0.0423
1	1	6	58.9850	59.4376	59.4855	-0.0479

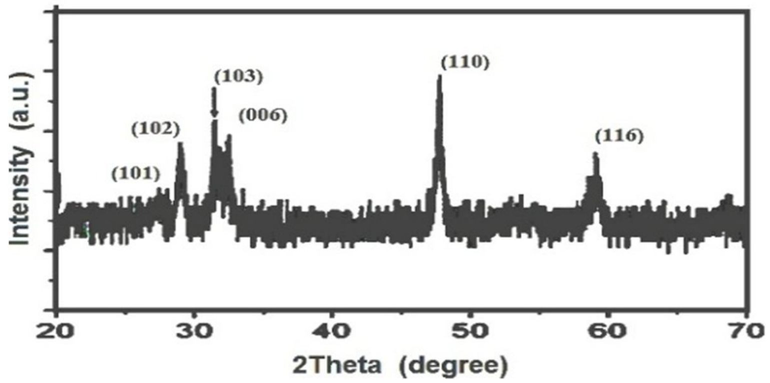

FIG. 1. P-XRD of CuS thin film compound.

The aim of XRD was only for the formation of compound and phase, since data was not suitable for deep structural study. However, we have estimated the size of grain (D) 14nm and the dislocation density (δ) 0.005032 nm^{-2} from the peak width (β_{hkl}) of good orientation. The microstructure strain (ε), due to imperfection and distortion (in crystal structure), is found 0.44, which is significant. All these parameters were calculated by using the following formulae and are given in Table 1.

Debye's formula -

$$D = \frac{K\lambda}{\beta_{hkl}\cos\theta} \quad (2)$$

$$\delta = \frac{1}{D^2} \quad (3)$$

$$\varepsilon = \frac{\beta_{hkl}}{4\tan\theta} \quad (4)$$

Where, k is the shape parameter which is 0.89 for spherical considerations, λ is the wavelength of x-ray of Cu-K_α and β_{hkl} is the peak width in radians.

TABLE 1. XRD results (unit cell refinement and analysis of microstructure).

Unit Cell and Microstructure	Parameter	Refined /Calculated Values
Lattice Constant	a & b	3.77(0.008) (Å)
	C	16.34(0.110)(Å)
Unit Cell Volume	V	201.57(1.434) (Å^3)
Unit Cell Density	D	4.74(gcm^{-3})
Microstructure	D	14±1.36 nm
	δ	0.005032 nm^{-2}
	ε	0.44±0.089

Note: Bracket () terms indicate deviation.

Optical Properties

Optical properties of CuS thin film are observed as the absorbance (A) and percentage of transmission (%T) (transmittance) parameters from the data obtained from the spectrometer and their characteristics are shown in Fig. 2 and Fig 3. The peak of absorbance is observed maximum just above 400 nm which is also conversely observed in %T. Data was post-processed for the absorption coefficient (α) and extinction coefficient (k) parameters and plotted as a function of photon energy as shown in Fig 4 and Fig 5. The maximum of absorption coefficient (peak) lied around 2.96 eV, whereas extinction coefficient's maximumlied around 2.64 eV. These 'α' and 'k' values are calculated from the relations given in Eq. (5) and in Eq. (6),respectively as follow.

$$\alpha = \frac{2.303\times A}{t} \quad (5)$$

$$k = \frac{\alpha\lambda}{4\pi} \quad (6)$$

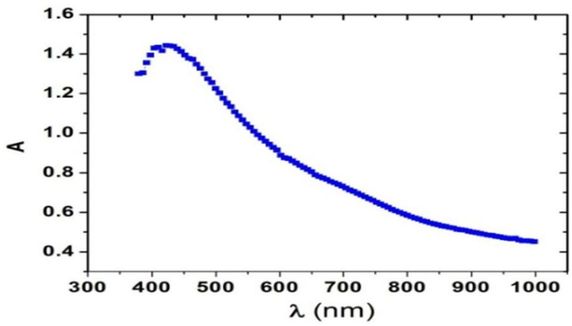

FIG. 2. Absorption spectrum of CuS thin film.

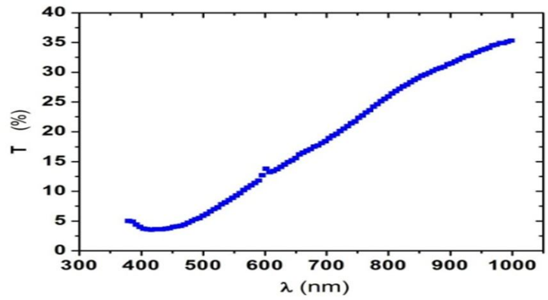

FIG. 3. Transmission spectrum in percentage.

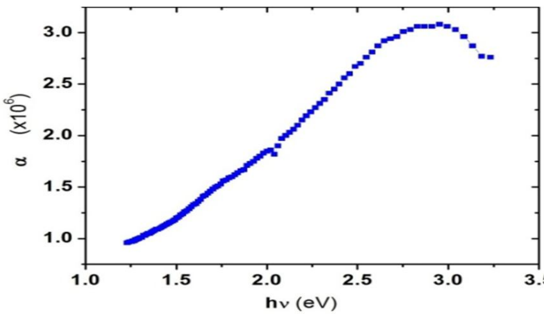

FIG.4. Absorption coefficient as a function of photon energy.

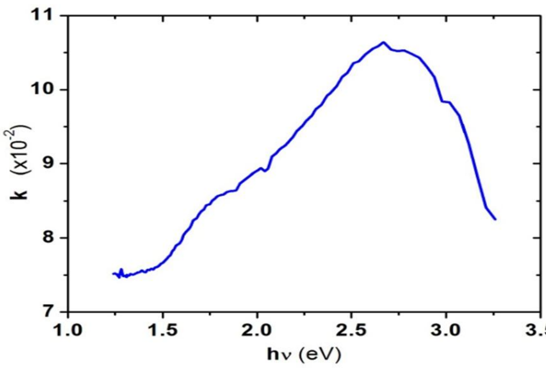

FIG.5. Extinction coefficient as a function of photon energy.

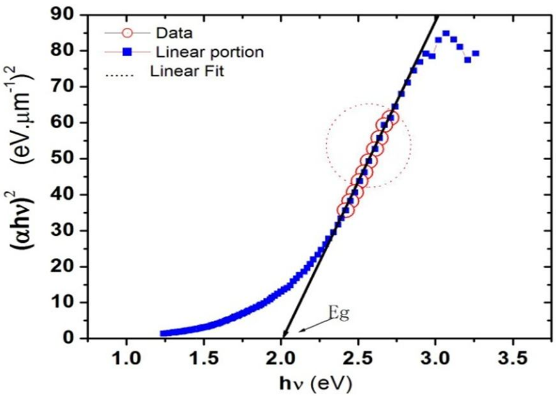

FIG. 6. Optical energy gap of CuS thin film.

An important characteristic property of material extracted from optical data is the energy band gap (Eg). Eg of CuS thin film is obtained from the x-intercept of an extrapolation of the linear part of the tail of data plotted in the graph in Fig. 6. The graph has been plotted $(\alpha.h\nu)^2$ *versus* photon energy representing Eq. (7) by (Tauc method) [7-15, 19].

$$(\alpha.h\nu)^2 = K(h\nu - Eg)^2 \tag{7}$$

where, ν = the frequency of radiation, h = Planck's constant, $h\nu$ is photon energy, K = constant. The allowed transition is possible for the found band gap of 2.01 eV which is non-interrupted by phonon. This Eg is in the order of reported 2.07 eV band gap in another work[18]. The transition in which the phonon vibrations of the lattice took part for the band gap can be tested by Eq. (8).

$$(\alpha.h\nu)^{\frac{1}{2}} = K(h\nu - Eg)^2 \tag{8}$$

But, it was avoided and is not presented in this paper due to the observed peak in Fig. 2 and the observed linear portion in Fig. 6. Probably, this implies that the thin film is free from impurities. Therefore, the CuS thin film possesses direct band gap energy and allows transition due to photon absorption only. We observe differences in the preparation method when compared with literature, such as that spray pyrolysis method gave lower-band gap thin film material compared to the chemical bath deposition and dip coating deposition synthesis methods which reported 2.2 eV for t=11nm and 2.5 eV for t=13nm, respectively[20]. Localized defect states are observed (which can effectively influence the conduction and valence bands' edges) from the presence of the Urbach tail (i.e, absorption tail). It is calculated in the form or Urbach energy [21], which is nothing but the slope of the Ln(α) *versus* hυ graph above the band gap energy region. It is found to be 313 meV.

Four-probe Electrical Study

Electrical response of thin film material at different temperatures has been obtained in four-probe experiment and used to calculate the bulk resistivity and the conductivity of CuS thin film. Conductivity is calculated from the reciprocal of the bulk resistivity and the bulk resistivity is calculated from the Voltage-Current (V-I) characteristics measured in a four-probe experiment using Eq. (9) [22].

$$\rho = 4.532\ \mathrm{t}\left(\frac{\mathrm{V}}{\mathrm{I}}\right) \tag{9}$$

where, t is thickness, V is voltage measured as a function of temperature and I is current kept constant at 0.49 μA and four-probe correction factor for thin film sheet is $\left(\frac{\pi}{\ln 2}\right) = 4.532 \times \mathrm{t}$.

The bulk resistivity and conductivity data plots are not seen smooth; instead, they are observed as steps. This is illustrated in Fig. S1 and Fig. S2 in the supplement. Data is significantly irregular at 320 to 330 K and around 360 K. But, for the full range of 300 to 380 K, the linear character is observable and hence we performed linear fit in resistivity case. The resistivity was found decreasing with increasing temperature with a rate of 1.5×10^{-5} Ωm/K, which determines the semiconducting nature. Fig. S2 reveals that the film has increasing conductivity, which supports literature [23]. For electrical property response, natural log of conductivity as a function of 1000/T was plotted and fitted to a straight line as shown in Fig 7 in accordance with Eq. (10).

$$\sigma = \sigma^{0} \exp\left(\frac{\mathrm{E_a}}{\mathrm{KT}}\right); \tag{10}$$

Where, E_a is the thermal activation energy and K is Boltzmann's constant. The data fitted showed decrement with reducing temperature. It does not show increment as the semiconducting to metallic transformation in one reported work [24]. The slope of graph is found to be -0.4618 which is$\left(\frac{\mathrm{E_a}}{\mathrm{KT}}\right)$. E_a is estimated to be 0.0398 eV from this. It is in good agreement with 0.03 eV of the silar-prepared 278 nm thick thin film having Eg= 2.28eV and grain size of 17 nm which has a resistivity of 0.05Ωcm at 303 K [25]. Using Hall effect method, Ea was estimated at 0.007 eV for 100°C and 0.013 eV for 150 and 200°C in case of 13nm grain size thin film.

Therefore, for the range of 300 to 380K, it is confirmed that the film is becoming more and more conductive as temperature rises upto 375K.

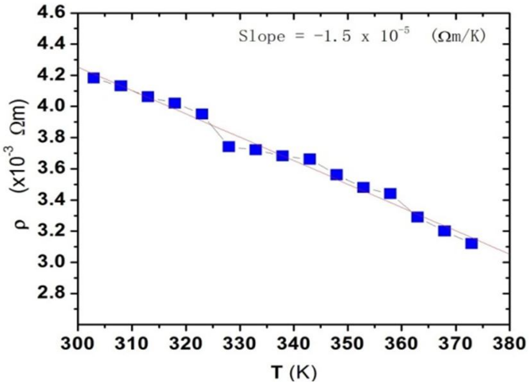

FIG. S1. Variation in electrical resistivity of CuS thin film.

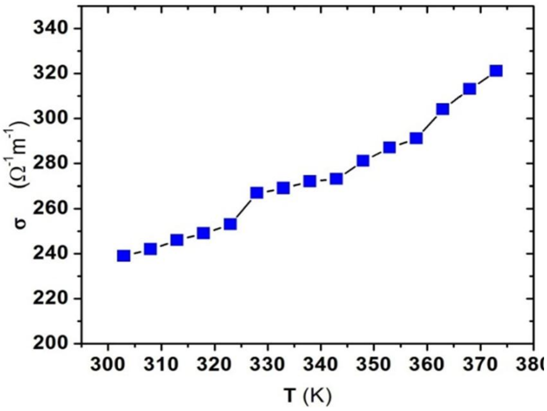

FIG. S2. Variation in electrical conductivity of CuS thin film.

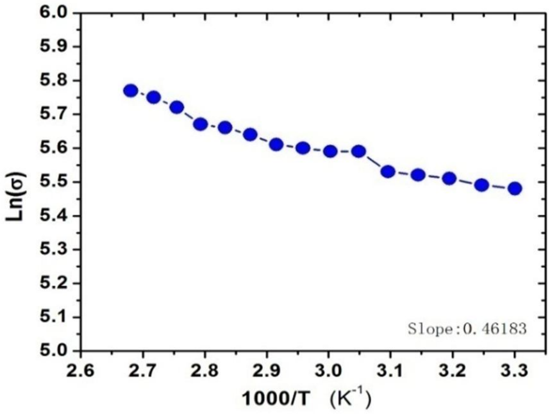

FIG.7.Natural log of conductivity as a function of (1000/T).

Morphology and Dielectric Properties

1- Morphology

All the above optical and electrical properties are concerned with film's material surface morphology. We have tracked it from the XRD data of FWHM (Full Width Half Maxima) of the peak in term of the morphological index (M.I.). M.I is calculated using the highest broadening $(FWHM_h)$ and particular broadenings$(FWHM_{hkl})$ by the following formula [26].

$$M.I. = \frac{FWHM_h}{FWHM_h + FWHM_{hkl}} \quad (11)$$

The smaller index to higher index (for eg. 0.5 to 0.99) refer the blocks to platue type morphologies as per[27]. In Cu thin film, we observed that M.I. is ranging from 0.5 to 0.59, as shown in Table 2 and found proportional to the crystallites domain size with a correlation coefficient of 0.9904. It shows good morphology which is tending toward uniformity at the size of grains/crystallites. Inter-planar spacing and size corresponding to particular orientations are also provided in Table 2.

TABLE 2: Plane spacings, morphology and grain size corresponding to particular (hkl) orientations.

hkl	d (Å)	Size (nm)	MI
(102)	3.036	15.27569	0.590
(103)	2.804	14.90345	0.583
(006)	2.725	14.16049	0.570
(110)	1.888	14.34639	0.561
(116)	1.553	11.79916	0.500

2-Optical Conductivity and Dielectric Constant

We extend our optical study to optical conductivity (σ_{opt}) by using the following formula:

$$\sigma_{opt} = \frac{\alpha n c}{4\pi} \quad (12)$$

Where, R is the reflectance of CuS thin film and c is the speed of light in SI unit. The$\sigma_{opt}$is plotted as a function of photon energy (shown in Fig. 8) illustrating that optical conductivity increases with photon energy up to 2.92 eV. Conductivity was found more at 423nm.

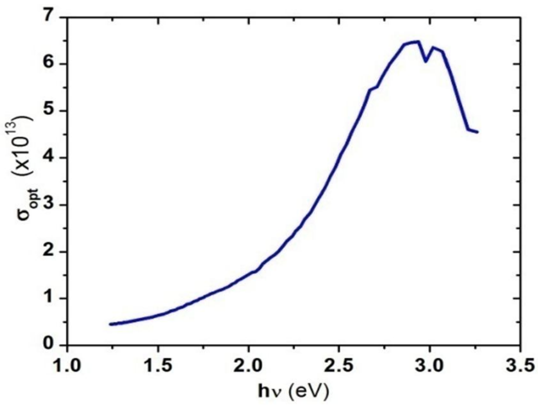

FIG.8. Optical conductivity as a function of wavelength.

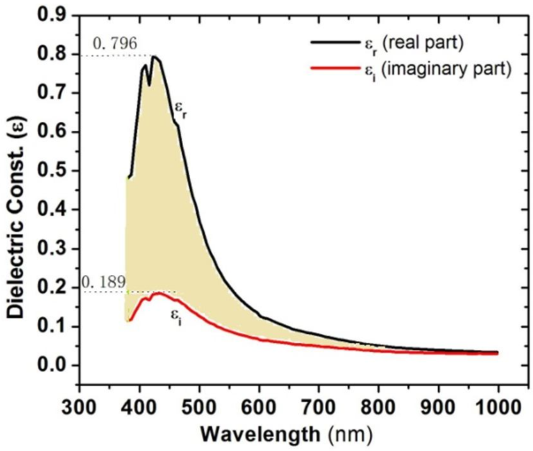

FIG.9. Dielectric constant variation with wavelength.

We have also examined the optical data for dielectric properties as shown in Fig. 9.It is characterized by real-part (ε_r) and imaginary-part (ε_i) constants which are calculated by the following formulae [27].

$$\varepsilon_r = n^2 + k^2 \tag{13}$$

$$\varepsilon_i = 2nk\ ; \tag{14}$$

where n is the refractive index calculated as per [27]. The real part of dielectric constant is maximum 0.796 at a wavelength of 423 nm and decreases toward the higher wavelength (lower photon energy). Compared to this, the imaginary part is maximum 0.189 at 432 nm and showsthe same decreasing phenomenon. Fig. 9 clearly identifies the comparison $\varepsilon_r > \varepsilon_i$and the difference between them reduces toward larger wavelengths.

Conclusion

The CuS thin film is successfully deposited on a glass slide at 380^{0}C by spray pyrolysis technique and observed as a good semiconductor. It is polycrystalline in nature and has a 14 nm grain size with unit cell of hexagonal symmetry. This work has reported 2.01 eV direct band gap energy with the presence of localized states for 1.0973μm film thickness at 380^{0}C substrate temperature. The optical study for the region 380 – 1000 nm revealed the good electronic nature of the CuS thin film material in terms of absorption, transmission character and optical constants. We are possibly the first to successfully present the immediately-characterized optical and electrical study of CuS thin films after synthesis and cooling. Electric conductivity is increasing and thermal activation occurred. Optical conductivity and dielectric constant also confirm the similar nature with photons for nearly uniform morphology of the film.

References

[1] Pathan, H.M. and Lokande, C.D., Bull. Mater. Sci., 27 (2004) 85.

[2] Sagadevan, S. and Murugasen P., International Journal of Chemtech Research, 6 (14) (2014) 5608.

[3] Dhawankar, S.H. and Suryavanshi, B.M., International Journal of Physical Research, 4(2) (2016) 58.

[4] Singh, A.K., Mehra, S. and Thool, G.S., European Chemical Bulletin, 2(8) (2013) 518.

[5] Dhawankar, S.H., Patil, A.K. and Suryavanshi, B.M., Applied Physics Letter, 1 (2) (2014).

[6] Kassim, A., Min, H.S., Haron, M.J. and Nagalingam, S., Int. J. of Pharm. & Life Sci., 2 (11) (2011) 1190.

[7] Isac, L.A., Duta, A., Kriza, A., Enesca I.A. and Nanu, M., Journal of Phys. Conf. Series, 61 (2007) 477.

[8] Thanikaikarasan, S., Mahalingam, T., Kathalingam, A., Moon, H. and Kim, Y.D., J. of New Materials for Electrochemical Systems, 12 (2009) 29.

[9] Alex, B.F., Martinson, S.C., Thimsen, R.E., Elam, J.W. and Pellin M.J., Energy and Environmental Science, 6 (2013) 1868.

[10] Dhawankar, S.H., Patil, A.K., Lad, J.S. and Suryavanshi, B.M., Scholars Research Library, Archives of Physics Research, 4(3) (2013) 7.

[11] Johansson, J., Kostamo, J., Karppinen, M. and Niinisto L., Journal of Material Chemistry, 12 (2002) 1022.

[12] Dhawankar, S.H., Patil, A.K., Lad, J.S. and Suryavanshi, B.M., International Journal of Innovative and Applied Research,2(8) (2014) 67.

[13] Wu, Y., Wadia, C., Ma, W., Sadtler, B. and Alivisatos, P., Nano Letters, 8(8) (2008) 2551.

[14] Sagade, A.A. and Sharma, R., Sensors and Actuators B, 133 (2008) 135.

[15] Dhawankar, S.H., Patil, A.K., Suryavanshi, B.M. and Tirpude, M.P., International J. of Phys. Res., 5(1) (2017) 1.

[16] Nascu, C., Pop, E., Ionescu, V., Indrea, E. and Bratu, I., Material Letters, 32 (1997) 73.

[17] Adelifard, M., Eshghi, H. and Mohagheghi M.M.B, Applied Surface Sci., 258 (15) (2012) 5733.

[18] Firat,Y.E., Yildrim,H., Erturk,K. and Peksoz,A., Scanning, 2017 (2017) 2625132.

[19] Tayade, N.T., Dhawankar, S.H. and Arjuwadkar, P.A., Journal of Physical Sciences, 22 (2017) 137.

[20] Chaki, S.H., Deshpande, M.P. and Tailor, J.P., Thin Solid Films, 550 (2014) 291.

[21] Grozdanov, E. and Najdoski, M., J. of Solid State Chem., 114(2) (1995) 469.

[22] Cruz, J.S., Hernandez, S.A.M., Delgado, F.P., Angel O.Z., Perez, R.C. and Delgado, G.T., International J. of Photoenergy, 2013 (2013) 9.

[23] Choudhury, B. and Chaudhary, A., Phys. E., 56 (2014) 364.

[24] Gaikawad, P.D., Shirale, D.J., Gade, V.K., Savale, P.A., Kharat, H., Kakade, K.P., Hussaini, S.S., Dhumane, N.R. and Shirsat, M.D., Bull. Mater. Sci., 29 (2006) 169.

[25] Ubale, A.U., Bhute, M.V., Malpe, G.P., Raut, P.P., Chipade, K.S. and Ibrahim S.G., J. of Saudi Chemical Society, 20(2) (2016) 227.

[26] Sarkar, S. and Das, R., Indian J. Pure and Appl. Phys., 56 (2018) 765.

[27] Jacob, R., Nair, H.G. and Isac, J., Int. Lets. Chem., Phys. and Astronomy,2 (2015) 100.